

Original Article

Arthritis Care & Research
DOI 10.1002/acr.23166**Running title: A prospective study of hip shape and OA****Hip shape as a predictor of osteoarthritis progression in a prospective population cohort**

¹Harbeer G. Ahedi, ²Richard M. Aspden DSc, ¹Leigh C. Blizzard Ph.D., ²Fiona R. Saunders Ph.D., ³Flavia M. Cicuttini Ph.D., ¹Dawn A. Aitken Ph.D., ¹Graeme Jones MD, and ²Jennifer S. Gregory Ph.D.

¹Menzies Institute for Medical Research, University Of Tasmania, Hobart 7000, Tasmania, Australia. ² Aberdeen Centre for Arthritis and Musculoskeletal Health, Institute of Medical Sciences, University of Aberdeen, Forester hill, Aberdeen, AB25 2ZD, United Kingdom.

³DEPM, Monash University, Victoria, Australia

HA was funded by an Australian Government Postgraduate Award, and this study was supported by an OARSI collaborative scholarship to HA and held in Aberdeen.

Address correspondence to:

Harbeer Ahedi,

Menzies Institute for Medical Research, University of Tasmania,

Private Bag 23, Hobart, Tasmania 7001, Australia

Phone +61 3 6226 4232

Fax: +61 3 6229 7704

Email: Harbeer.Ahedi@utas.edu.au

This article has been accepted for publication and undergone full peer review but has not been through the copyediting, typesetting, pagination and proofreading process which may lead to differences between this version and the Version of Record. Please cite this article as an 'Accepted Article', doi: 10.1002/acr.23166

© 2016 American College of Rheumatology

Received: Jun 09, 2016; Revised: Nov 18, 2016; Accepted: Dec 06, 2016

ABSTRACT

Objective: Hip morphology plays a significant role in the incidence and progression of hip osteoarthritis (OA). We hypothesized that hip shape would also associate with other key factors and tested this in a longitudinal community-based cohort combining radiographic, MRI, DXA, and clinical data.

Methods: Baseline dual-energy X-ray absorptiometry (DXA) images of the left hip of 831 subjects from the Tasmanian Older Adult Cohort (TASOAC) were analyzed using an 85-point statistical shape model. Hip pain was assessed by WOMAC (Western Ontario and McMaster Universities Osteoarthritis Index) and muscle strength was measured by a dynamometer. Hip structural changes were assessed using MRI and Radiographic OA (ROA) using plain radiographs.

Results: Six shape modes described 68% of shape variation. At baseline, modes 1, 2, 4 and 6 were associated with hip ROA, modes 1, 3, 4 and 6 correlated with hip cartilage volume and all except mode 2 with muscle strength. Higher mode 1, and lower mode 3 and 6 scores at baseline predicted hip pain at follow-up and higher mode 1 and mode 2 scores were associated with hip effusion-synovitis. Greater scores for mode 2 (decreasing acetabular coverage) and lower mode 4 (non-spherical femoral head) at baseline predicted 10-year total hip replacement (THR); while mode 4 alone correlated with bone marrow lesions (BMLs), effusion-synovitis, and increased cartilage signal.

Conclusions: Hip shape is associated with ROA, THR, hip pain, effusion-synovitis, BMLs, muscle strength and hip structural changes. These data suggest that different shape modes reflect multiple facets of hip osteoarthritis.

SIGNIFICANCE AND INNOVATIONS

- Scores from statistical shape models from baseline DXA images of the hip in a longitudinal population cohort are strongly associated with total hip replacement ten years later.
- Baseline measures of hip shape were strongly associated with hip pain, hip bone marrow lesions (BMLs), hip cartilage volume, larger hip effusion-synovitis, increased cartilage signal, hip ROA, over a five-year period.
- Early pistol-grip-deformity correlates with hip BMLs, hip effusion-synovitis size, lower cartilage volume and lower leg strength.
- Hip morphological features are associated with key clinical, radiographic and structural factors relevant for the incidence and progression of OA and provide a basis for identifying and monitoring early hip OA. This will enable early modifications to diet and exercise to benefit the patient, as well as assist clinicians and companies seeking to reduce the time taken to test new therapeutics.

Osteoarthritis(OA) is a musculoskeletal disorder that affects the elderly population around the globe and imposes a considerable economic burden on society (1). Although OA is a disease of the whole joint, bone and cartilage still remain the focus of its clinical manifestation (2). Structural changes such as bone marrow lesions (BMLs) and cartilage defects are linked with progression of hip OA (3-6). In addition to these, the morphology of the hip can predict the development of hip OA (7), but most current assessments are semi-quantitative and focus on changes in the cartilage and the presence of bony outgrowths (8, 9). However, subtle morphological changes are difficult to detect by predefined geometrical measures, which do not capture the total morphology of the hip.

Statistical shape modelling (SSM) (10) is a sophisticated technique that yields a quantitative measure of hip morphology from two-dimensional images of the joint, such as radiographs (7), and can identify subtle shape variation within a population. An SSM generates a set of linearly independent ‘modes of variation’, each of which describes a coordinated pattern of variation in hip shape within a study group. Each mode has a mean of zero and unit standard deviation (SD). Every image is then assigned a score for each mode describing how many standard deviations it lies from the mean. For instance, in a longitudinal study using radiographs from the Rotterdam study, subjects who had low scores for mode 6 (describing the upper femoral neck with a sharper transition from the femoral head into the lower femoral neck) at baseline were at higher risk of developing severe hip OA and total hip replacement (THR) (7). Subsequently, we have shown that SSM can be used to model DXA (dual-energy x-ray absorptiometry) images (11, 12) and that Kellgren-Lawrence grading can be applied to these images with as much precision as to radiographs (13). In another longitudinal, nested, case-controlled study of elderly women, hip

shape modes specifically reflecting sizes of the femoral head, femoral neck or greater trochanter modestly predicted hip OA (14). Moreover, hip shape modes could also predict THR independently of clinical, geometrical and radiological factors (15). However, shape modes describing radiographic OA (ROA) may not necessarily associate with clinical descriptors such as pain or crepitus (16, 17). Hence, different shape modes might be better at predicting either clinical or radiological progression of hip OA and may differ between males and females as they have different hip and pelvic shapes (18).

OA is a multifactorial disease and it is unknown to what extent morphological aspects of the hip relate to disease progression. Studies to date have shown that SSM is a powerful quantitative tool and is sensitive to changes in bone shape (7, 14-16, 19, 20), but it has not been used to study hip OA in a large community-based cohort and has not previously been tested for associations with BMLs or effusion-synovitis. Thus, the aim of this study was to describe the association between hip shape measured at baseline and clinical, demographical, structural and radiological features of hip OA both at baseline and over time in an older adult Australian cohort using a combination of radiographic, MRI, DXA and patient questionnaire data.

SUBJECTS AND METHODS

Subjects. The Tasmanian Older Adult Cohort (TASOAC) study is an ongoing prospective, population-based study initiated in 2002. A total of 1,100 subjects were enrolled in the study between March 2002 and September 2004 (phase 1). Follow-up data for three clinic visits (phase 2, 3 and 4) were collected for 875, 769 and 568 participants respectively. These visits were conducted approximately 3 years, 5 years and 10 years from baseline.

A total of 1099 subjects attended a clinic for baseline measurements. Of these, 264 subjects did not have a DXA image and images for 4 subjects were corrupted, leaving 831 subjects with complete baseline data. The hip joint shape was measured from baseline DXA scans. All other measures were collected from clinical visits or questionnaires between baseline and the 5 years (phase 3) follow-up apart from THR which was recorded up to 10 years (phase 4) (Supplementary Figure 1). Written informed consent was obtained from all participants and the Southern Tasmanian Health and Medical Human Research Ethics Committee approved this study.

Demographic characteristics, medical history, and lifestyle factors were assessed by self-administered questionnaires. Height and weight were measured and body mass index (BMI) calculated using standard protocols (21). At each follow-up assessment, participants were asked if they had undergone total hip replacement surgery and in which hip.

Hip pain. At baseline, the self-reported hip pain was recorded as yes/no using a standardized questionnaire. The presence and severity of hip pain for all the subjects at the follow-up visits for phases 2 and 3 were determined using a hip-specific Western Ontario and McMaster Universities Osteoarthritis (WOMAC) index pain score (22).

Muscle strength. Muscle strength (leg strength) was measured at each visit to the nearest kilogram-force in both legs simultaneously, using a dynamometer (TTM Muscular Metre, Tokyo, Japan) as described previously (23).

Magnetic resonance imaging (MRI). The right hip was imaged in the sagittal plane during visits at phases 2 and 3 using a 1.5 Tesla GE Signa whole-body magnetic resonance scanner with a phased-array flex-coil using two sequences. Sagittal plane imaging was chosen to facilitate the quantitative analysis described below.

Sagittal images were obtained at a partition thickness of 1.5 mm with an in-plane resolution of 0.39 x 0.39 mm (512 x 512 pixels) (24) using, a T1-weighted, fat-suppressed, 3-dimensional gradient-recalled acquisition in the steady state. The parameters for this were: flip angle 55 degrees; repetition time 58 ms; echo time 12 ms; inversion time (IT) 130 ms; field of view 16 cm; 60 partitions; 512 x 512-pixel matrix; acquisition time 11 mins 56 s, and one acquisition.

The second set of sagittal images was obtained with a slice thickness of 3.5 mm and an inter-slice gap of 1.5 mm (4) using a STIR (Short T1 Inversion Recovery)-weighted, fat saturation, two-dimensional fast spin-echo sequence. This sequence used a repetition time 4340 ms, echo time 28.4 ms; field of view 20 cm; 15 partitions (16 slices) and 512 x 512-pixel matrix.

Hip cartilage volume. Baseline femoral head cartilage volume was measured for each individual from the T1-weighted images using the software program Osiris (Windows version 3.5; Geneva University Hospital, Geneva, Switzerland). The volume of the femoral head cartilage was calculated by manually drawing contours around the cartilage boundaries on each image section. These data were then resampled by bilinear and cubic interpolation for the final 3D rendering. Intra-observer reliability was assessed and the coefficient of variation (CV) was 2.5% (24).

Hip bone marrow lesions (BML). Quantitative assessment of subchondral hip BMLs in STIR MRI images was done using OsiriX software (Mac version, University of Geneva, Geneva, Switzerland). BMLs were identified as areas of increased signal intensity adjacent to the subchondral bone on the femoral head and/or the acetabulum (3, 4).

High cartilage signal. High cartilage signal was identified as an increase in the signal intensity of the articular cartilage due to increased water content that appears as a bright band in the cartilage either adjacent to a hip BML or at any location on the STIR MRI slice if there was no BML present (25, 26). High cartilage signal was graded as 0 for absent and 1 for present (3, 4).

Hip effusion-synovitis. Hip effusion-synovitis was identified and assessed in STIR images from phase 2 and phase 3. The observer (HA) manually selected the MR slice with the largest effusion-synovitis and determined the maximum cross-sectional area (CSA) of the bright region by manually drawing contours around the outer edges. In a reliability study of 40 subjects with re-measurements after four weeks, the intra-rater agreement (kappa) for presence of hip effusion-synovitis was 0.84, and the ICC (3, 1) for hip effusion-synovitis CSA was 0.97.

Radiological assessment. Anteroposterior radiographs of the pelvis were obtained at the first visit with the individual weight-bearing and with both feet internally rotated by 10 degrees. Radiographs were read by two trained readers using the OARSI (Osteoarthritis Research Society International) grading system. Radiographic features of joint space narrowing (JSN) (axial and superior) and osteophytes (superior acetabular and femoral) of both hips were graded separately on a 4-point scale, ranging from 0 to 3 where 0=no disease and 3=most severe disease. A non-zero score of either JSN or osteophytes was regarded as evidence of hip ROA. Thus, after combining JSN and osteophytes score, the presence of hip ROA was defined as a total score of 1 or greater in the left hip for comparison with the DXA images.

DXA imaging and statistical shape modelling (SSM). At phase 1, DXA images were taken of the left hip using a Hologic Delphi scanner. Images were extracted from the Hologic data files using custom-made Matlab software (Math Works Inc, Natick, United States) and saved as 8-bit BMP files.

An 85-point SSM was built to assess the shape of the femoral head, acetabulum and femoral neck using the Active Shape Modelling toolkit (University of Manchester, Manchester, UK). This model included not only the femoral head but also osteophytes and the acetabulum and extended down the upper femoral diaphysis to include cortical thickness. The SSM template is a set of landmark points that define the shape to be identified. For comparison between images, each point is always placed on the same anatomical feature on the outline of the bone (Supplementary Figure 2).

The coordinates of the points were collected and transferred to custom-written SHAPE software (University of Aberdeen, UK). Using SHAPE, the data underwent Procrustes transformation, to remove size and orientation effects, and were subjected to principal components analysis to

generate an independent set of orthogonal mode scores for each image (16). The distribution of each mode is normalized to zero mean and unit standard deviation so that the scores assigned to each image are in units of standard deviations. Reference to a 'lower' score, therefore, implies a position towards the more negative end of the distribution rather than smaller in absolute terms. A scree plot was generated to visualize the variance described by each mode.

A set of 10 images were selected at random from the dataset and the points placed on the images by two independent observers (HA & FRS). Point-to-point variability (the distance between equivalent points placed by each observer) was calculated. The distribution was not normal and the median was 1.6 pixels.

Statistical analyses. Characteristics of the population were summarized as means and standard deviations or as percentages and frequencies. At baseline, the associations of hip shape mode scores with the presence of hip pain and radiographic features were assessed using log-binomial regression analyses. Pairwise Pearson's correlations were used to calculate the correlations of hip shape mode scores with age, body mass index (BMI), hip cartilage volume and leg strength while a generalised linear model was applied to calculate the link between hip shape mode scores and sex. Follow-up data from all phases were combined for analysis to identify any OA-related changes at any subsequent stage following recruitment and longitudinal associations of baseline hip shape with the presence of hip pain, MRI-based structural findings and THR were explored using log- binomial regression. Linear regression analyses were used to investigate the longitudinal associations of baseline mode scores with hip pain severity. Pairwise correlation coefficients were calculated between hip shape, hip BMLs, and effusion-synovitis size. All models were adjusted for age, sex, and body mass index (BMI). Correlations between repeated measurements on individuals were taken into account by adjusting standard errors using the sandwich (robust) estimator of variance (27-29). All statistical analyses were performed using Intercooled STATA 12 (Stata Corp, College station, Texas, USA).

RESULTS

Characteristics of the sample population are presented in Table 1. From the shape of the scree plot, the first six shape modes were selected. The shape variations described by each mode of the six modes of variation are shown Supplementary Table 1 and variations in the modes with most frequent associations modes 1, 2, 4 and 6 are shown in Figure 1. These six modes explained 68% of the total variation in the population and all were greater than 3.5%. Mode scores for males and females separately are shown in Supplementary Table 2 and mode 2 was the only mode not

associated with sex. Prevalence ratios for males to females were for mode 1, PR = 0.84 ($P < 0.001$), men had, on average, higher mode 1 scores than females, while higher scores for modes 3-6 were more common among females (range of PR:1.16-1.35, $P < 0.001$).

Self-reported hip pain at baseline was not associated with hip shape (Table 2) but modes 2 and 6 were associated with the presence of hip ROA. Further analysis of the components of hip ROA showed that lower scores of modes 1 and 2 were weakly associated with the presence of JSN and lower mode 4 scores were associated with increased prevalence of osteophytes. Mode 6 was positively associated with the major features of ROA with each standard deviation increase in score corresponding to a 23%, 15% and 13% greater prevalence of JSN, osteophytes, and hip ROA, respectively.

Correlations of hip shape modes with age, BMI, leg strength and baseline MRI-based structural findings are presented in Table 3. Age at baseline was significantly associated with lower mode 2 scores, describing a wider neck, loss of joint space and greater femoral head coverage. Lower scores for modes 1-4 were modestly correlated with greater BMI. Greater mode 1 scores, along with lower scores for modes 3-6, were associated with greater leg strength and greater hip cartilage volume.

Although not associated with the presence of hip pain at baseline, hip shape was associated with the presence and severity of hip pain at follow-up (Table 4). Higher mode 1 scores and lower scores for modes 3 and 6 predicted an increase in prevalence of hip pain at follow-up. Mode 3 score was also negatively associated with the severity of hip pain.

Shape modes 2 and 4 at baseline also correlated with MRI-based hip structural changes at follow-up and with subsequent THR (Table 5). Mode 2 was strongly and positively associated

with increased prevalence of THR; a 1 SD increase in score indicating a 60% increase in prevalence. Mode 4 was strongly and negatively associated with the presence of both BMLs and high cartilage signal, and a reduction of 1 SD in mode 4 score indicated a 40% increase in both the prevalence of THR and the presence of BMLs. A diagrammatic summary of the significant associations between mode scores and prevalence may be found in Supplementary Figure 3.

DISCUSSION

This study links the predictive power of SSM, for quantifying the shape of the hip, with ROA, THR, BMLs, effusion-synovitis, pain and anthropometric data. A particular strength is the application of SSM to a population-based cohort to compare a quantitative description of joint shape at baseline with comprehensive participant data from MRI, radiographs, and DXA images as well as questionnaire data at baseline and over the following 10-years. In this way we have identified features of hip shape that are associated with both the incidence and the progression of hip OA.

In this cohort, whose average age was 63 at enrollment, nearly 40% already reported hip pain. At follow-up, the proportion with hip pain increased slightly and over the ten years, 29 subjects underwent THR. Morphological variation was found between males and females with higher scores for mode 1 and lower scores for modes 3-6 being more common in males. Mode 1 represents the largest variation in shape and higher scores are associated with increasing head size and femoral neck length and width (Supplementary Table 1). During follow-up, MRI showed that about one-fifth of the cohort had a hip BML whereas about three-quarters had a high cartilage signal and most showed signs of hip effusion-synovitis.

Baseline

Leg strength and radiographic features.

Interestingly, these modes had similar associations with greater hip cartilage volume and leg strength, even after correction for sex. Associations with hip ROA were largely negative and no association was found with hip pain. Lower mode 1 scores, for instance, indicating a shorter, narrower femoral neck, were associated with greater joint space narrowing. Surprisingly, although osteophytes could be included in the SSM, none of these first six modes showed any variation in the location of the points marking the positions of osteophytes although modes 4 and 6 were both associated with the presence of osteophytes as seen in the radiographic scoring.

Decreasing scores for mode 2 identified characteristics such as increasing acetabular coverage, a smoother transition of the upper femoral head into the femoral neck and an increasingly non-spherical femoral head which may indicate a pistol-grip-like deformity and femoro-acetabular impingement (8). At baseline, a lower score for this mode associated with greater prevalence of both JSN and ROA. Lower scores of mode 4, with prominent features of pistol-grip deformity, along with higher mode 6 scores, which represented those with a flatter femoral head, shorter femoral neck and sharp transition of the femoral head into the neck were associated with a greater prevalence of osteophytes. Associations of shape modes with hip ROA have been previously published and variations in the shape of the femoral head, its transition into the superior aspect of the neck and the length of the femoral neck have been reported to be associated with risk of hip ROA (7, 14-18).

Follow-up

Hip pain and shape modes. Higher baseline scores of mode 1 and lower scores of mode 6 were associated with incident hip pain at follow-up. Lower mode 3 scores were associated with greater prevalence and severity of hip pain. Lower scores of mode 3 indicate a shorter femoral neck and sharp transition of the lower femoral head into femoral neck. Previous studies have shown that morphological variations in the femoral neck are predictive of hip pain (16, 30). Modes 1 and 6 were associated not only with radiographic features (at baseline), but mode 1 also correlated with hip effusion-synovitis CSA at follow-up. These factors might explain the associations of these modes with hip pain. Overall, our results are consistent with previous studies that have demonstrated associations between shape modes and hip pain (16, 18)

Structural changes and hip shape. Modes 2 and 4 appear to associate strongly with structural changes in the subchondral bone of the hip which are risk factors for progression of OA (3, 4). For instance, at baseline, lower scores of these modes associated with greater JSN and prevalence of osteophytes respectively. Similarly, at follow-up, a low score for mode 4 predicted OA-related features such as higher probability of the presence of BMLs, high cartilage signal and correlated with larger BML and hip effusion-synovitis size. In contrast, greater values for mode 2 were found to be associated with effusion-synovitis. Features highlighted by both these modes correspond to cam deformity and pistol-grip deformity, which are well-known risk factors for the development of hip OA (8, 31). As this is the first study to identify the link between hip shape and structural changes such as BMLs, there are no previous data exploring the association; these morphological features could encourage structural changes in the subchondral bone and cartilage (7, 14, 15, 18).

Higher scores of both modes 1 and 2 modestly correlated with larger effusion-synovitis CSA and a +1 SD higher mode 2 score predicted a 22% greater prevalence of the presence of hip effusion-synovitis. In further analyses, longitudinal associations were found between baseline shape and change in hip effusion-synovitis (from phase 2 to phase 3). Over this period, a one SD lower baseline mode 1 score was associated with greater hip effusion-synovitis CSA (β : -0.20; 95%CI: -0.30, -0.06), whereas no association was found with mode 2. Mode 1 thus appears to be predictive not only of hip pain but also hip effusion-synovitis and future studies will explore whether this is an early indicator of later ROA as suggested by other studies (32).

Total hip replacement and shape modes. The same two modes that associated most strongly with MRI structural features, modes 2 and 4, also showed the strongest associations with hip replacement. Increasing mode 2 and decreasing mode 4 scores strongly associated with THR. Every 1 SD increase in mode 2 score increased the risk of THR by about 60% and a -1 SD change in mode 4 increased the risk of THR by about 40%. Both these modes identified shape patterns related to OA such as the transition of the femoral head into the femoral neck, the size of the greater trochanter a flattening of the femoral head itself and mode 2 captured coverage of the femoral head by the acetabulum (16). Overall, excessive coverage of femoral head by the acetabulum, also known as femoral-acetabular impingement (FAI), along with features related to pistol-grip deformity are known to associate with greater risk of hip OA (8, 31, 33).

A number of limitations need to be noted. This study uses DXA images of the left hip while MRI-detected anomalies were measured in the right hip, so the joint appearances may not be directly comparable. Nevertheless, it has been demonstrated that OA in the ipsilateral joint strongly predicts and associates with OA in the contralateral joint and studies using SSM have reported similar results (34). The effect of the internal / external rotation of the femur, arising

from variations in patient positioning, cannot be ruled out and even when using standardized protocols in which the position of the feet is carefully controlled, this might influence the DXA images. Nevertheless, SSM has the potential to pick up the effects of rotation from the variation in shape during the development of the model (7, 16, 20). Point placement on identifiable landmarks is important to define the model and is a potential source of error. After initial manual placement on a small number of images, the SSM is a semi-automated program which uses points at defined locations to measure the global shape of the hip joint. Each image is checked by the user and points adjusted if visually incorrect. The small point-to-point error is an indicator of placement of points by different observers to within a few pixels.

In summary, in this population-based study, two-dimensional hip shape measured on entry to the study is shown to be associated with ROA and muscle strength at baseline. More interestingly, shape is also strongly predictive of THR, as well as indicators of OA such as hip pain, BMLs, effusion-synovitis and hip structural changes occurring up to 10 years later. These data suggest that different morphological features identified by shape modes have relevance for multiple facets of hip osteoarthritis, both radiographic and clinical. It adds further evidence for the use of SSM as an imaging biomarker for the incidence and progression of OA. Where standardized radiographs or DXA images are available we believe that in due course it may be possible to include a measure of shape into clinical imaging practice for the early detection and staging of OA.

Conflict of Interest

The authors have no conflict of interest.

Acknowledgements

A special thanks go to the participants of the TASOAC study. We thank Catrina Boon and Pip Boon for their contributions.

Funding sources

The TASOAC study was supported by the National Health and Medical Research Council of Australia, Tasmanian Community Fund, Masonic Centenary Medical Research Foundation, Royal Hobart Hospital Research Foundation and Arthritis Foundation of Australia. This project was funded by OARSI (Osteoarthritis Research Society International) collaborative scholarship.

REFERENCES

1. Cross M, Smith E, Hoy D, Nolte S, Ackerman I, Fransen M, et al. The global burden of hip and knee osteoarthritis: estimates from the Global Burden of Disease 2010 study. *Ann Rheum Dis*. 2014;annrheumdis-2013-204763.
2. Aspden RM. Osteoarthritis: a problem of growth not decay? *Rheumatology (Oxford, England)*. 2008;47(10):1452-60.

3. Ahedi H, Aitken D, Blizzard L, Cicuttini F, Jones G. The association between hip bone marrow lesions and bone mineral density: a cross-sectional and longitudinal population-based study. *Osteoarthr Cartil.* 2013;19(13):838-8.
4. Ahedi H, Aitken D, Blizzard L, Cicuttini F, Jones G. A population-based study of the association between hip bone marrow lesions, high cartilage signal, and hip and knee pain. *J Clin Rheumatol.* 2013;33(3):369-76.
5. Neumann G, Mendicuti AD, Zou KH, Minas T, Coblyn J, Winalski CS, et al. Prevalence of labral tears and cartilage loss in patients with mechanical symptoms of the hip: evaluation using MR arthrography. *Osteoarth Cart.* 2007;15(8):909-17.
6. Teichtahl AJ, Wang Y, Smith S, Wluka AE, Giles GG, Bennell KL, et al. Structural changes of hip osteoarthritis using magnetic resonance imaging. *Arthritis Res Ther.* 2014;16(5):466.
7. Gregory JS, Waarsing JH, Day J, Pols HA, Reijman M, Weinans H, et al. Early identification of radiographic osteoarthritis of the hip using an active shape model to quantify changes in bone morphometric features: can hip shape tell us anything about the progression of osteoarthritis? *Arthritis Rheum.* 2007;56(11):3634-43.
8. Micheal Doherty PC, Sally Doherty, Wendy Jenkins, Rose A Maciewicz, Kenneth Muri and Weiya Zhang. Nonspherical Femoral Head Shape (Pistol grip deformity), Neck-Shaft Angle, and Risk of Hip Osteoarthritis *Arthritis Rheum.* 2008;58(10):3172-82.
9. Kasper K Goving SJ, Stig Sonne-Holm. Prevalence of malformations of the hip joint and their relationship to sex, groin pain and risk of osteoarthritis: A population-based survey. *J Bone Joint Surg.* 2010;92-A(5):1162-9.
10. Cootes TFTC. Active Shape Models. Hogg D BR, editor. Berlin Germany Springer-Verlag 1992.
11. Yoshida K, Barr RJ, Gregory JS, Aspden RM, Alesci S, Macfarlane GJ, et al. Link Between the Severity of Osteoarthritis and the Shape of the Hip Joint Using DXA Images. *Rheumatol.* 2009;48:I99-I.
12. Yoshida K, Gregory JS, Barr JR, Alesci S, Aspden RM, Reid DM. Temporal structural changes in hip OA detected using Shape and Appearance modelling of DXA images: a One-Year Prospective Cohort Study. *Osteoarth Cart.* 2009;17 Supplement 1:S24.

13. Yoshida K, Barr RJ, Galea-Soler S, Aspden RM, Reid DM, Gregory JS. Reproducibility and Diagnostic Accuracy of Kellgren-Lawrence Grading for Osteoarthritis Using Radiographs and Dual-Energy X-ray Absorptiometry Images. *J Clin Densitom.* 2015;18(2):239-44.
14. Lynch NP, Chaganti RK, Nevitt MC, Lane N. The association of proximal femoral shape and incident radiographic hip OA in elderly women. *Osteoarthr Cartil.* 2009;17:1313-8.
15. Barr RJ, Gregory JS, Reid DM, Aspden RM, Yoshida K, Hosie G, et al. Predicting OA progression to total hip replacement: can we do better than risk factors alone using active shape modelling as an imaging biomarker? *Rheumatology (Oxford).* 2012;51(3):562-70.
16. Waarsing JH, Rozendaal RM, Verhaar JN, Bierma-Zeinstra SA, Weinans H. A statistical model of shape and density of the proximal femur in relation to radiological and clinical OA of the hip. *Osteoarthr Cartil.* 2010;18:787-94.
17. Agricola R, Reijman M, Bierma-Zeinstra SM, Verhaar JA, Weinans H, Waarsing JH. Total hip replacement but not clinical osteoarthritis can be predicted by the shape of the hip: a prospective cohort study (CHECK). *Osteoarthr Cartil.* 2013;21(4):559-64.
18. Nelson AE, Liu F, Lynch JA, Renner JB, Schwartz TA, Lane NE, et al. Association of incident symptomatic hip osteoarthritis with differences in hip shape by active shape modeling: the Johnston County Osteoarthritis Project. *Arthritis Care Res (Hoboken).* 2014;66(1):74-81.
19. Goodyear SR, Barr RJ, McCloskey E, Alesci S, Aspden RM, Reid DM, et al. Can we improve the prediction of hip fracture by assessing bone structure using shape and appearance modelling? *Bone.* 2013;53(1):188-93.
20. Gregory JS, Testi D, Stewart A, Undrill PE, Reid DM, Aspden RM. A method for assessment of the shape of the proximal femur and its relationship to osteoporotic hip fracture. *Osteoporos Int.* 2004;15(1):5-11.
21. Ding C, Cicuttini F, Boon C, Boon P, Srikanth V, Cooley H, Jones G. Knee and hip radiographic osteoarthritis predict total hip bone loss in older adults: A prospective study. *J Bone Miner Res.* 2010;25:858-65.
22. Bellamy B, Buchanan W, Goldsmith C, Campbell J, Stitt L. Validation study of WOMAC: a health status instrument for measuring clinically important patient relevant outcomes to antirheumatic drug therapy in patients with osteoarthritis of the hip or knee *J Rheumatol.* 1988;15(12):1833-40.

23. Scott D, Blizzard L, Fell J, Jones G. Prospective associations between ambulatory activity, body composition and muscle function in older adults. *Scand J Med Sci Sports*. 2011;21(6):1600-0838.
24. Zhai G, Cicuttini F, Srikanth V, Cooley H, Ding C, Jones G. Factors associated with hip cartilage volume measured by magnetic resonance imaging: the Tasmanian Older Adult Cohort Study. *Arthritis Rheum*. 2005;52(4):1069-76.
25. Totterman S, Tamez-Pena J, Schreyer E, Gonzalez P, Hunter DJ. Cartilage-bone contrast behavior in OAI progression sub-cohort: correlation to WOMAC scores. *Osteoarthr Cartil*. 2009;17 Suppl 1:S74-S5.
26. King L, Higgs J, Aisen A, Buckwalter K, Martel W, McCune J. MRI in osteoarthritis of the hip: Gradiations of severity. *Magn Reson Imaging*. 1988;6:229-36.
27. Huber P, editor *The behavior of maximum likelihood estimates under nonstandard conditions*. Proceedings of the Fifth Berkeley Symposium on Mathematical Statistics and Probability; 1967; Berkeley, California, USA: Univerisity of California Press.
28. White H. A Heteroskedasticity-Consistent Covariance Matrix Estimator and a Direct Test for Heteroskedasticity. *Econometrica*. 1980;48(4):817-38.
29. Rogers W. Regression standard errors in clustered samples. *Stata Technical Bulletin*. 1993;13:19-23.
30. Nelson AE, Golightly YM, Liu F, Lynch J, Gregory JS, Aspden RM, et al. Variations in hip shape are associated with radiographic knee osteoarthritis: cross-sectional and longitudinal analyses of the Johnston County Osteoarthritis Project. *J Rheumatol*. 2015;In press.
31. Agricola R, Heijboer MP, Bierma-Zeinstra SM, Verhaar JA, Weinans H, Waarsing JH. Cam impingement causes osteoarthritis of the hip: a nationwide prospective cohort study (CHECK). *Ann Rheum Dis*. 2013;72(6):918-23.
32. Bierma-Zeinstra SM, Bohnen AM, Verhaar JA, Prins A, Ginai-Karamat AZ, Lameris JS. Sonography for hip joint effusion in adults with hip pain. *Ann Rheum Dis*. 2000;59(3):178-82.
33. Gosvig KK, Jacobsen S, Sonne-Holm S, Gebuhr P. The prevalence of cam-type deformity of the hip joint: a survey of 4151 subjects of the Copenhagen Osteoarthritis Study. *Acta Radiol*. 2008;49(4):436-41.

34. Sayre EC, Jordan JM, Cibere J, Murphy L, Schwartz TA, Helmick CG, et al. Quantifying the association of radiographic osteoarthritis in knee or hip joints with other knees or hips: the Johnston County Osteoarthritis Project. *J Rheumatol.* 2010;37(6):1260-5.

Accepted Article

Table 1. Characteristics of the TASOAC cohort at baseline and follow-up. Data from all follow-up visits were combined to identify features of OA at any stage subsequent to recruitment.

Characteristics	Mean (S.D) (n=831)
Baseline	
Age (yrs.)	63.2 (7.45)
Sex (Males)	49%
Body Mass Index (BMI)	27.7 (4.63)
Hip cartilage volume (mm ³)	5340 (1100)
Presence of hip pain (Y/N)	42%
Radiological hip OA (ROA) (Y/N)	41%
Follow-up	
Presence of hip pain (WOMAC) (Y/N)	47%
Hip pain score (WOMAC)	2.60 (5.24)
Leg strength (kg)	93.1 (48.5)
Presence of hip bone marrow lesions (BMLs) (Y/N)	18%
Hip BML area (cm ²)	0.20 (0.52)
Presence of hip cartilage defects (Y/N)	72%
Presence of high cartilage signal (Y/N)	74%
Presence of hip effusion-synovitis (Y/N)	95%
Hip effusion-synovitis area (cm ²)	1.96 (1.60)
Total hip replacement (Y/N) *	2.64%

Data presented as means and standard deviations or percentages and frequencies

* Includes all hip replacements (left or right) from all follow-up assessments

Accepted Article

Table 2. The associations of hip shape with hip pain, JSN and radiographic hip OA at baseline. Prevalence ratios and 95% confidence intervals adjusted for age, sex and body mass index at baseline. Bold text represents $P < 0.05$.

Mode	Hip pain	JSN	Osteophytes	Hip ROA
	<i>PR (95%CI)</i>	<i>PR (95%CI)</i>	<i>PR (95%CI)</i>	<i>PR (95%CI)</i>
1	1.03 (0.92, 1.14)	0.88 (0.78, 0.99)	0.94 (0.82, 1.09)	0.94 (0.84, 1.05)
2	0.99 (0.90, 1.11)	0.76 (0.70, 0.85)	1.05 (0.91, 1.22)	0.85 (0.76, 0.95)
3	0.97 (0.90, 1.08)	0.96 (0.85, 1.09)	1.09 (0.94, 1.26)	0.98 (0.90, 1.11)
4	0.97 (0.90, 1.08)	1.03 (0.91, 1.17)	0.79 (0.70, 0.92)	1.07 (0.95, 1.20)
5	1.04 (0.93, 1.17)	0.93 (0.83, 1.06)	0.94 (0.81, 1.09)	0.93 (0.82, 1.04)
6	0.96 (0.90, 1.07)	1.23 (1.09, 1.40)	1.15 (1.00, 1.33)	1.13 (1.01, 1.27)

Table 3. Correlations of hip shape mode scores with age, BMI, leg strength and hip cartilage volume at baseline. Correlations with leg strength and hip cartilage volume were adjusted for age, sex and body mass index. Significant values are presented as bold text. * $P < 0.05$, ** $P < 0.01$ and

Mode	Age (yrs.)	BMI (kg/m ²)	Leg strength (kg)	Hip cartilage Volume (cm ³)
1	-0.04	-0.12^{***}	0.20^{***}	0.40^{***}
2	-0.13^{***}	-0.07[*]	0.00	-0.03
3	-0.03	-0.11^{***}	-0.15^{***}	-0.20[*]
4	-0.04	-0.10^{***}	-0.13^{***}	-0.25^{***}
5	-0.04	-0.04	-0.22^{***}	-0.13
6	-0.04	-0.02	-0.13^{***}	-0.21[*]

*** $P < 0.001$

Table 4. Associations of hip shape modes at baseline with presence and severity of hip pain at follow up. Prevalence ratio PR (95%CI) and β co-efficient (95% CI) all adjusted for age, sex and body mass index with clustering of observation on subjects at phases 2 and 3 taken into account.

Mode	Presence of hip pain PR (95% CI) *	Severity of hip pain β (95% CI)**	Bold denotes $P < 0.05$.
1	1.09 (1.00, 1.20)	0.17 (-0.20, 0.55)	
2	0.99 (0.91, 1.09)	-0.13 (-0.50, 0.21)	
3	0.91 (0.82, 0.99)	-0.43 (-0.84, -0.02)	
4	0.99 (0.90, 1.09)	-0.12 (-0.55, 0.30)	
5	1.03 (0.94, 1.14)	0.10 (-0.24, 0.45)	
6	0.91 (0.84, 0.99)	-0.05 (-0.40, 0.30)	

Table 5. Associations of hip shape modes at baseline with MRI based structural findings and total hip replacement (THR) at follow up. Prevalence ratio PR (95%CI) and correlation coefficients (r) (95% CI) all adjusted for age, sex and body mass index with clustering of observation on subjects at phases 2 and 3 taken into account. Bold denotes statistically significant results. * $P < 0.05$, ** $P < 0.01$ and *** $P < 0.001$.

Mode	Presence of hip				BML	Effusion-
	Presence of any hip BMLs	Presence of high cartilage signal	effusion-synovitis ≥ 2 sites	THR	area (cm ²)	synovitis area (cm ²)
	PR (95%CI)	PR (95%CI)	PR (95%CI)	PR (95%CI)	r	r
1	1.30 (0.92, 1.81)	1.03 (0.92, 1.20)	1.12 (0.91, 1.40)	0.84 (0.63, 1.12)	0.06	0.20 ***
2	1.22 (0.89, 1.70)	1.06 (0.96, 1.20)	1.22 (1.00, 1.50)	1.60 (1.20, 2.15)	0.08	0.21 ***
3	1.12 (0.82, 1.52)	1.04 (0.93, 1.15)	0.95 (0.77, 1.20)	0.75 (0.60, 1.00)	-0.00	-0.10
4	0.60 (0.42, 0.82)	0.89 (0.80, 0.99)	1.13 (0.92, 1.41)	0.63 (0.50, 0.84)	-0.13 *	-0.11 *
5	0.82 (0.60, 1.14)	1.02 (0.91, 1.15)	0.88 (0.72, 1.08)	1.34 (0.99, 1.80)	-0.09	0.07
6	0.90 (0.62, 1.30)	0.97 (0.87, 1.08)	0.91 (0.71, 1.20)	0.96 (0.72, 1.30)	-0.07	0.00

Figure Legends

Figure 1. Showing the variation in shape for +2 (solid red) and -2 (dashed blue) standard deviations in mode score from the mean of zero for modes 1, 2, 4 and 6. Descriptions of the key features identified by each mode are given Supplementary Table 1.

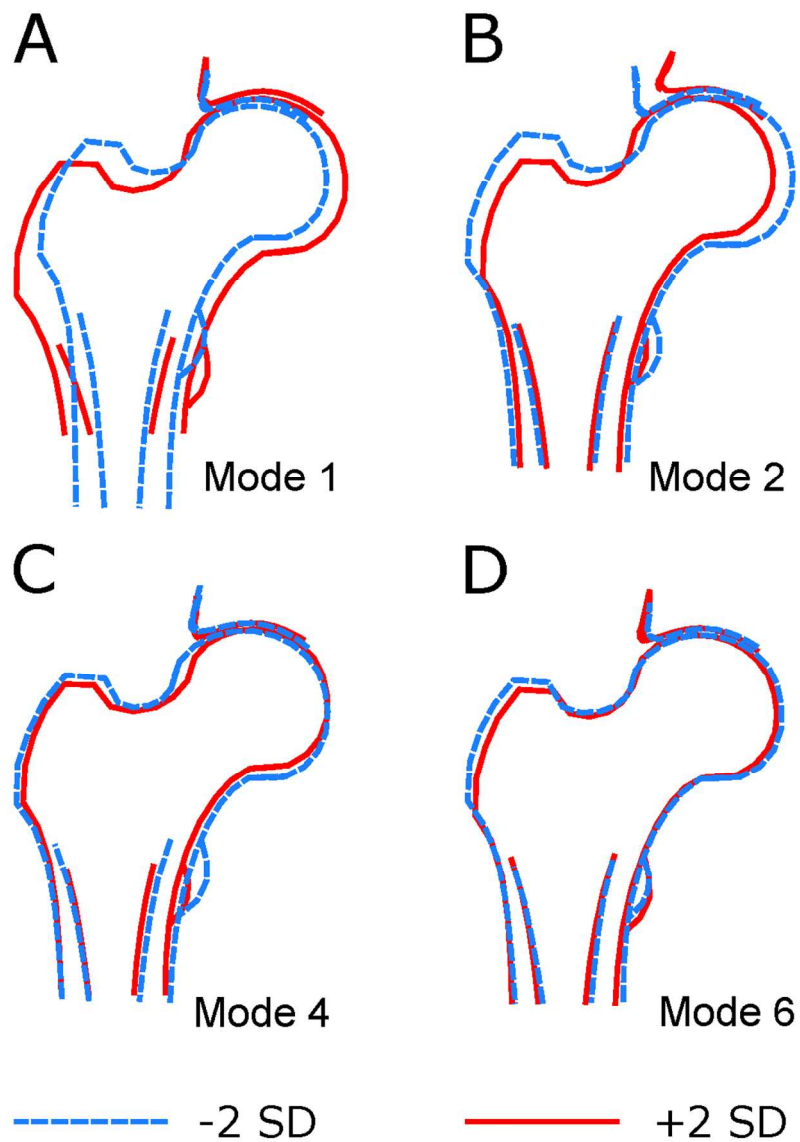


Figure 1. Showing the variation in shape for +2 (solid red) and -2 (dashed blue) standard deviations in mode score from the mean of zero for modes 1, 2, 4 and 6. Descriptions of the key features identified by each mode are given Supplementary Table 1.

170x201mm (200 x 200 DPI)

A